Dynamic Multipath Model of Low Angle Passive Radar Tracking with Experimental Evaluation

Yu-liang Qin[*] and Yong-qiang Cheng

National University of Defense Technology, Changsha - 410 073, China
[*]*E-mail: qinyuliang@nudt.edu.cn*

ABSTRACT

The problem of multipath propagation encountered in radar tracking of low elevation targets in the presence of reflections from the sea is addressed. A detailed model of the multipath propagation considering both the specular and the diffuse reflection components in target tracking using passive radars is established. Based on the geometry of the specular and the diffuse reflections, expressions for the reflection coefficient and the scattering field are derived. Experiments in the outfield indicate that the model proposed agrees with the test data well, which can provide an accurate prediction of the angle measurement errors in the presence of multipath effects.

Keywords: Multipath propagation effect, low-altitude target tracking, specular reflection, diffuse reflection

1. INTRODUCTION

In tracking low elevation targets, the presence of reflections from the sea (or ground) surface (i.e., multipath propagation) can cause severe errors in the target angle measurement, which brings a great influence on the overall tracking performance. Estimation or prediction of the multipath error is normally a difficult task due to the complexity of the reflection properties of the surface as well as the dependency of this error on a large number of radar parameters.

In the past, multipath effects in radar tracking have been studied by many researchers. Beckman and Spizzichino[1], put forward the classic theory applied to the far-field diffuse reflection on rough surface, and established the concept of flashing surface. Then, Barton analysed the radar measurement error due to the diffuse reflection on rough surface, and pointed out that the radar echo is a random variable which complies with a definite probability distribution (usually the Rice distribution) [2]. In the early 1990s, Bruder studied the fixed deviation in the indicated target angle due to the specular reflection on the flat surface[3]. Sletten and Trizna[4], *et al*. carried out an experiment to investigate the multipath propagation over the sea surface in the purpose of analysing its implications for sea-clutter statistics.

Along with the study of the reflection characteristics, a number of different methods including angle averaging, frequency agility, offset angle track were presented and a combination of these methods was suggested to reduce the effects of multipath. For example, the multipath propagation was considered as an estimation/tracking problem and a filtering technique was employed to reduce the multipath effects[5]. In continuation, the use of frequency agility and the fusion of the tracks obtained with different waveform frequencies were presented[6]. Then, a maximum maneuver-based filter

and a multiple model estimator were proposed to compensate the multipath error in tracking with monopulse radars[7]. Recently, several new techniques are introduced to reduce the interference of multipath effects, such as orthogonal frequency division multiplexing (OFDM)[8-9], blind signal separation[10] and Fractional Fourier Transform (FrFT)[11]. However, due to the complexity of the problem itself, there are still many issues to be studied.

In multipath effects, the modelling of the multipath propagation is a fundamental problem. In earlier works, researchers mainly focus on the reflection characteristics of the rough surface in low-angle radar tracking. For the actual tracking scenes, especially for tracking low elevation targets over the sea, there are few models providing detailed description of the multipath errors due to reflections of the three-dimensional sea surface. In this paper, a dynamic model of the multipath propagation considering both the specular and the diffuse reflection components in target tracking using passive radars is established. The two components of the sea surface reflection are described. A three-dimensional description of the sea surface is introduced based on the sea spectrum model. Then, based on the geometry of the specular and the diffuse reflections, expressions for the reflection coefficient and the scattering field are derived. The result of simulations of the dynamic sea surface is presented. The proposed model is validated by the test data of experiments in the outfield, which indicates that the model provides an accurate prediction of the angle measurement errors in the presence of multipath effects.

2. MULTIPATH PROPAGATION OF THE SEA SURFACE

When tracking low elevation targets, the presence of reflections from the sea surface can result in a strong interference

in target angle measurements. A simple illustration of the geometry of multipath propagation is depicted in Fig. 1. There are two separate paths between the target and the passive radar: the direct path and the indirect path via reflections with grazing angle from the sea surface. The incident complementary angle of the direct path is α. The surface reflected signal generally consists of two components, namely, specular (coherent) and diffuse (incoherent). The specular reflection is caused by a smooth (mirror-like) surface with grazing angle θ while the diffuse reflection is caused by the surface irregularities. The incident complementary angle and the reflective complementary angle of the diffuse signal are θ_1 and θ_2, respectively.
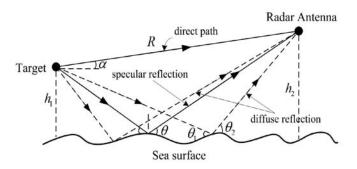

Figure 1. Geometry of the multipath propagation.

To study the multipath effects of the sea, a three-dimensional model of the sea surface is required. Then, three components of the received signal of radar antenna (i.e. the direct incident signal, the specular reflection signal and the diffuse reflection signals) need to be calculated. In the calculation of diffuse reflection signals, the sea surface is divided into finite small panels by orthogonal rectangular. Firstly the diffuse signals for each of the small panels are calculated. Then, according to the geometry of the diffuse reflection, whether the reflected signals can be received by the radar antenna is determined. All the diffuse signals which can be received are summed to obtain the total diffuse signal. Finally, the three components of the received signal of radar antenna are vectorially summed to calculate the target angle. The calculation flow chart of the sea multipath propagation is depicted in Fig. 2.
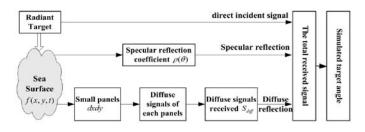

Figure 2. Calculation flow chart of sea multipath.

3. THREE-DIMENSIONAL MODEL OF THE SEA SURFACE

The sea surface is formed by the interactions of the sea wind, the sea gravity and the sea surface tension, while such interactions are nonlinear and changing with time.

The sea surface is approximately cyclical in large-scale and superimposed on small-scale ripples. That is to say, it is a blend with both large-scale structure and micro-structure[12-13]. The methods of simulating the sea surface can be mainly divided into two categories: Fractal simulation and statistical simulation. As the spectrum of fractal function is a negative power-law spectrum, it can only construct a rough surface obeying the negative form of power-law spectrum, while the statistical simulation method can construct any forms of spectrum. Therefore, the statistical methods are more generally used to simulate the sea surface.

The sea spectrum model is one kind of the statistical simulation methods. This method considers the waves as superimposed results of an infinite number of sine waves with ranged amplitude, frequency, direction and phase. The theory of random process and the linear wave's theory are used to analyze the sea spectrum. For the actual sea surface, its energy distributes not only in a certain frequency range, but also in a wide direction range. It can be regarded as a superposition of a number of cosine waves, with amplitude a_n, frequency ω_n, original phase ϕ_n and along with the spread direction angle θ_n. The expression of the spectrum can be denoted as

$$f(x, y, t) = \sum_{n=1}^{\infty} a_n \cos[\omega_n t - k_n (x \cos\theta_n + y \sin\theta_n) + \phi_n] \quad (1)$$

where k_n is the wave number of the nth component, and $-\pi \leq \theta_n \leq \pi$.

When there are only gravity waves, the frequency ω_n can also be expressed by the wave number[14] k_n

$$\omega_n^2 = g k_n^2 \quad (2)$$

The direction spectral density function of the sea spectrum is

$$S(\omega, \theta) d\omega d\theta = \sum_{\Delta\omega} \sum_{\Delta\theta} \frac{1}{2} a_n^2 \quad (3)$$

Theoretically, the range of θ is $-\pi \sim \pi$. However, actually the energy of waves usually distributes at $-\pi/2 \sim \pi/2$ which centered on the main spread direction. The direction spectral density function is generally of the following form:

$$S(\omega, \theta) = S(\omega) G(\omega, \theta) \quad (4)$$

where $S(\omega)$ is the spectrum function, $G(\omega, \theta)$ is the directional distribution function. There have been a number of perfect directional distribution functions. The spectrum function can be expressed using the angular frequency as follows[14]

$$S(\omega) = \frac{ag^2}{\omega^2} \exp[-\beta(\frac{g}{U\omega})^4] \quad (5)$$

where U represents the wind speed at the height of 19.5m of the sea, a is a constant which characterizes the height of the waves, and $a = 8.10 \times 10^{-3}$, g denotes the acceleration of gravity, β is a constant related with the average cycle and U, $\beta = 0.74$. The spectrum peak can be denoted as $\omega_m = 8.565/U$.

4. MODEL OF MULTIPATH PROPAGATION FORM SEA

4.1 Model of Specular Reflection

Figure 3 shows the geometry of the specular reflection from

sea, where T denotes the radiant source with the coordinates $(0, 0, h_1)$, a_1 and a_2 represent the passive radar antennas with the baseline which is d meters long, and the altitude of antennas is h_2. Taking the antenna a1 for example, the distance between T and a_1 is R, the angle between the direct signal and the centerline of the radiation beam is α, the distances between specular reflection point I and T, a_1 are R_1 and R_2, respectively. The angles between reflection signal and the centerline of the T, a_1 are α_1 and α_2, respectively, the grazing angle of the reflection surface is θ .
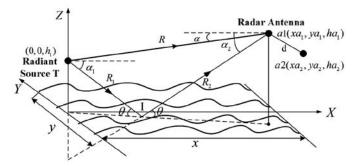

Figure 3. Geometry of the specular reflection from sea.

The distance R between the radiant source T and the antenna a_1 is

$$R = \sqrt{(xa_1^2 + ya_1^2 + (ha_1 - h_1)^2)} \tag{6}$$

The angle between the direct path Ta_1 and the beam axis of the radiant source is the coordinates of the specular reflection point I is

$$XI = \frac{R_1 \cos\theta}{\sqrt{(xa_1^2 + ya_1^2)}} xa_1, \ YI = \frac{R_1 \cos\theta}{\sqrt{(xa_1^2 + ya_1^2)}} ya_1 \tag{7}$$

$$\alpha = \arccos(\frac{xa_1}{\sqrt{xa_1^2 + ya_1^2 + (ha_1 - h_1)^2}}) \tag{8}$$

The angle between the specular incident component TI and the reflection surface is

$$\theta = \arctan(\frac{h_1 + ha_1}{\sqrt{(xa_1^2 + ya_1^2)}}) \tag{9}$$

The angle between the specular incident component TI and the beam axis of the radiant source is

$$\alpha_1 = \arccos(\frac{XI}{\sqrt{XI^2 + YI^2 + h_1^2}}) \tag{10}$$

The angle between the specular reflection component Ia_1 and the beam axis of the antenna a_1 is:

$$\alpha_2 = \arccos(\frac{xa_1 - XI}{\sqrt{(xa_1 - XI)^2 + (ya_1 - YI)^2 + ha_1^2}}) \tag{11}$$

The Fresnel reflective coefficient of the vertical polarization incident wave is

$$\rho_0(\theta) = \frac{\varepsilon \sin\theta - \sqrt{(\varepsilon - \cos^2\theta)}}{\varepsilon \sin\theta + \sqrt{(\varepsilon - \cos^2\theta)}} \tag{12}$$

The dielectric constant of sea water for the X-band incident waves is $\varepsilon = 60.4 - j32.4$.

The specular reflection factor ρ_s characterizes the attenuation rate of amplitude of the specular reflection due to the rough reflecting surface, and it has the following relationship with roughness factor Γ of reflecting surface[15].

Consequently, the total specular reflection coefficient can be calculated by

$$\rho(\theta) = \rho_0(\theta)\rho_s(\theta) \tag{13}$$

4.2 Model of Diffuse Reflection

The model of the diffuse reflection of the sea is presented on the basis of three-dimensional model of the sea surface. Firstly, the effective reflection region between the radiant source and the radar antenna are divided by finite two-dimensional orthogonal rectangles. Consequently, the actual terrain is reduced to a series of small panels with random gradient and random height. Then the diffuse signal of each of the small panels is calculated, which will be summed to obtain the total diffuse signal. The geometry of the diffuse reflection from sea is shown in Fig. 4.
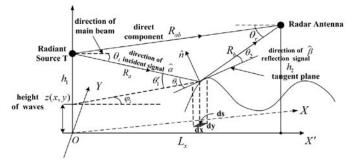

Figure 4. Geometry of the diffuse reflection from sea.

For the scattering of large-scale gravity waves, its dispersion field can be calculated by the Kirchhoff Approximate (KA) method, that is to say, the field of any point on the rough surface can be approximated by the field of the partial tangent plane around the scattering point. The area of panels can be approximately replaced by the projection ds on the plane when the panels are small enough.

The scattering field of the radar wave of the unit sea surface can be represented as follows[16]

$$E_{mn} = \frac{f_t(\theta_t)f_r(\theta_r)(\hat{n}\cdot\hat{q})\exp[jw_c(t-t_s)]\Delta x \Delta y}{4\pi R_a R_b n_z} V(\theta_1) \tag{14}$$

where L_x represents the horizontal distance between the radiant source and the radar, h_1 is the height of the radiant source, h_2 is the height of the radar antenna. For a point on the sea, the height of the waves is represented by $f(x,y)$, according to the results of three-dimensional simulation of the sea.

The angle between the incident component and the beam axis of the radiant target is θ_t, the angle between the diffuse reflection component and the beam axis of passive radar is θ_r, the pattern factors of the target's antenna and the radar antenna are $f_t(\theta_t)$ and $f_r(\theta_r)$ respectively; the incident complementary angle of the signal on the unit sea surface is θ_1, similarly, θ_2 is the reflective complementary angle; θ_1' denotes the angle between the incident waves and the x-y plane, θ_2' denotes the

angle between the reflective waves and the x-y plane; $V(\theta_1)$ is the scattering coefficient of the sea, R_a, R_b are the distances between (x, y) and the target and radar, respectively, R_{ab} is the distance between the target and radar; Δx, Δy are the lengths of the two sides of the panels, $\hat{n}$ is the unit normal vector of the panels, k is wave number, $\hat{\alpha}$ is the normal vector of the incident component, $\hat{\beta}$ is the normal vector of the reflective component, and $q = k(\hat{\beta} - \hat{\alpha})$.

The model parameters above are calculated as follows:

The diffuse reflection coefficient of sea

$$V(\theta_1) = \frac{\widehat{P_1} \cdot \hat{n}}{\cos^2 \theta_1} \left\{ V_V \cos(2\theta_1) \cdot (\hat{n} \cdot \widehat{P_2}) - \sin \theta_1 \cdot V_V \cdot (\hat{\alpha} \cdot \widehat{P_2}) \right\} \tag{15}$$

The incident complementary angle of the signal on the unit sea surface θ_1 is

$$\sin(\theta_1) = -\hat{\alpha} \cdot \hat{n} \tag{16}$$

The normal vector of the incident wave $\hat{\alpha}$ is denoted by:

$$\hat{\alpha} = (\cos \theta_1' \cos \varphi_1, \cos \theta_1' \sin \varphi_1, -\sin \theta_1') \tag{17}$$

While the unit normal vector of the panels $\hat{n}$ is:

$$\hat{n} = \left(\frac{K_1}{\sqrt{1 + K_1^2 + K_2^2}}, \frac{K_2}{\sqrt{1 + K_1^2 + K_2^2}}, \frac{1}{\sqrt{1 + K_1^2 + K_2^2}} \right) \tag{18}$$

The slopes K_1, K_2 of point (x, y) on the tangent plane towards x-axis and y-axis can be approximated by

$$K_1 = -\frac{\partial z}{\partial x} \approx -\frac{z(x_{m+1}, y_n) - z(x_{m-1}, y_n)}{2dx}$$

$$K_2 = -\frac{\partial z}{\partial y} \approx -\frac{z(x_m, y_{n+1}) - z(x_m, y_{n-1})}{2dy} \tag{19}$$

Substituting Eqns. (17), (18) and (19) into Eqn (16), the incident complementary angle can be denoted by:

$$\sin(\theta_1) = -\frac{\cos \theta_1'(K_1 \cos \varphi_1 + K_2 \sin \varphi_1) + \sin \theta_1'}{\sqrt{1 + K_1^2 + K_2^2}} \tag{20}$$

The normal polarization vectors of the incident wave and the reflective wave are

$$\widehat{P_1} \cdot \hat{n} = \frac{\sin \theta_1'(K_1 \cos \varphi_1 + K_2 \sin \varphi_1) + \cos \theta_1'}{\sqrt{1 + K_1^2 + K_2^2}} \tag{21}$$

$$\hat{n} \cdot \widehat{P_2} = -\frac{\sin \theta_2'(K_1 \cos \varphi_2 - K_2 \sin \varphi_2) + \cos \theta_2'}{\sqrt{1 + K_1^2 + K_2^2}} \tag{22}$$

$$\hat{\alpha} \cdot \widehat{P_2} = -\cos \theta' \sin \theta_2' \cos(\varphi_1 + \varphi_2) - \sin \theta_1' \cos \theta_2' \tag{23}$$

Finally, the total diffuse signal can be calculated by summing all the diffuse signals which can be received by the radar antenna

$$S_{diff} = \sum_{m=1}^{M} \sum_{n=1}^{N} E_{mn} \tag{24}$$

where M, N are the numbers of the effective panels towards x-axis and y-axis, respectively.

5. SIMULATION AND EXPERIMENTAL RESULTS

All the simulations in this section are implemented using MATLAB on an Intel Pentium 3GHz Dual-Core CPU, and 2GB RAM computer, while the test data are obtained by the experiments in the outfield using an X-band passive radar.

5.1 Dynamic Sea Surface

According to the wind speed of the sea surface, generally the sea surface can be classified as six kinds: wavelet, light waves, middle waves, big waves, billows and fierce waves. Based on the three-dimensional model of the sea, two typical situations of the sea (wavelet, light waves) are compared with simulations.

Figure 5 shows the simulation results of the dynamic sea surface under two wind speeds (5 m/s and 10 m/s). The parameters of the simulations are as follows: the ranges of the frequency ω are 1.2~6.0 rad/s and 0.4~2.5 rad/s, respectively. The stepping frequency intervals $\Delta\omega$ are 0.2 rad/s and 0.1 rad/s, respectively. The numbers N of harmonics are 24 and 21, respectively, while the simulation regions of the sea surface are

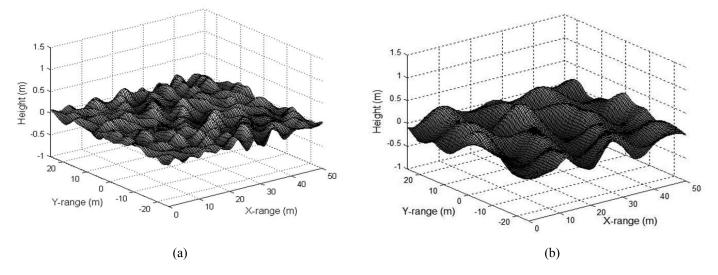(a)   (b)

Figure 5. Simulation results of the dynamic sea surface (a) wind speed - 5 m/s and (b) wind speed - 10 m/s.

both $(0 \sim 50)m \times (-20 \sim 20)m$.

From the comparisons between the results of the dynamic sea surface under two wind speeds, it can be seen that the conditions of the sea change significantly with the wind speed, which will result in different influence on the multipath effects. The undulant extent of the sea surface is small with relatively stable waves when the wind speed is 5 m/s, while the undulant extent is increasing when the wind speed is 10 m/s and the waves are wandering in the wave crest and trough. The simulation results illustrate that the low-frequency spectrum of waves are significant increasing when the wind speed increases which is consistent with the actual situations of the sea.

5.2 Results in the Outfield

In the outfield experiment, an X-band passive radar which is placed on the seawall is used to take measurements of the microwave radiant source placed on the target ship. The target ship moves from near to far relative to the detector (the X-band radar). The microwave interferometer is used to measure the angle of the target. The length of baseline between two antennae of the passive radar is 0.146 m. The gain of the antenna is 20 dB. The 3 dB width of the microwave radiant source and the radar antenna are 17° and 60°, respectively. The initial distance between the microwave radiant source and the radar is 1 km, while the total test distance is 14 km. The wind speed on the sea is 7 m/s (light waves) and the speed of the ship is 5 m/s. The heights of the radar antenna and the microwave radiant source are 8.2 m and 4.1 m, respectively. The radar works under the low-elevation tracking state. The experiment scenery in the outfield is illustrated in Fig. 6.
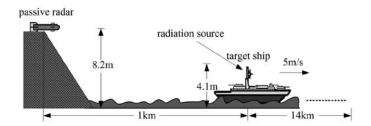

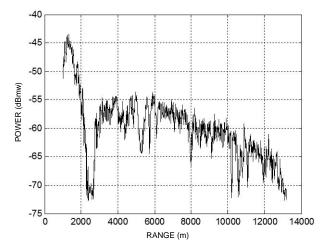Figure 6. Experiment scenery in the outfield.

Figure 7. Power – range curve of the received signal.

In the experiment, the power – range curve of the received signal is given in Fig. 7. A spectrum analyzer placed on the seawall is used to measure the power of the received signal. The unit of the signal power is dBmw. The measurements indicate that during the experiment, the power of the received signal encountered two significant drops: one is at 2 km due to the influence of multipath effects and the other is after 9 km which is caused by the serious signal loss.

5.3 Evaluation of the Model of Multipath Propagation

The outfield test data measures the power of the signals received by the passive radar. In the test radar, there is a fixed ratio between the voltages of received signal and the angle of target, which is 0.3 volts per degree. According to such a ratio, the angle measurement of the target can be calculated by the power of the received signals, while the true angle of the target can be calculated from the geometry of the experiment. On the other hand, the estimation or prediction results of the multipath propagation can be obtained based on the model proposed in this paper. Therefore, the model can be validated by the test data.

Comparison between the results of predictions of the multipath propagation based on the multipath model and the results of experiments are presented. Figure 8 gives three simulated components of the signals received by two antennae of the passive radar. The signals of each radar antenna are vectorially summed to calculate the target angle. Figures 9 - 11 give three comparisons between the predictions of the target angle in the presence of the multipath reflections from the sea and the angles measured in the experiment. The three comparisons consider only specular reflection, diffuse reflection and all the two components of reflections, respectively. The x-axis in the figures denotes the distance between the target and the radar antenna, while the y-axis denotes the elevation angle of the radiant source (in degrees).
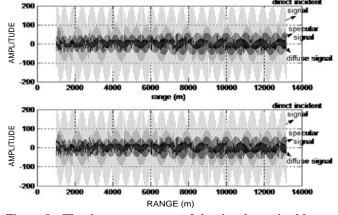

Figure 8. The three components of the signals received by two antennae of the passive radar.

In the simulations, Fig. 9 shows that the angle simulated according to the proposed model has a big drop at 2 km when only the specular reflection is considered, which agrees with the test data well. It changes gently at the other regions and has no oscillations. Figure 10 shows that the angle simulated is consistent with the measured angle of target when only the diffuse reflection is considered. There is no fixed bias. However,
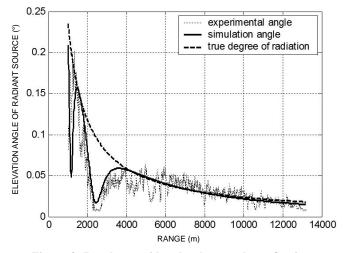
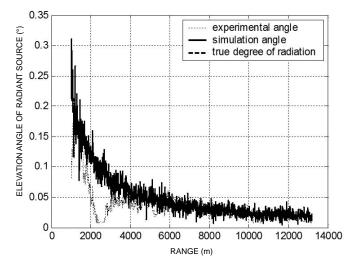**Figure 9. Results considered only specular reflection.**

Figure 10. Results considered only diffuse reflection.

the diffuse reflection component causes oscillations to the angle measurement, and reduces the measurement accuracy. Figure 11 shows that when all the two components are considered, the model provides an accurate prediction of the angle measurement errors in the presence of multipath effects.
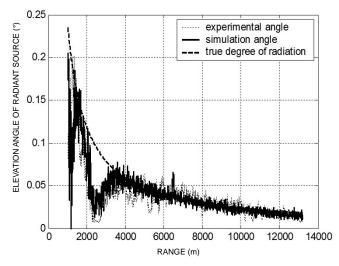

Figure 11. Results considered all of the reflection components.

The three simulations presented above indicate that the specular reflection causes large peak errors followed by an approximately constant bias in tracking low elevation targets in the presence of multipath reflections, while the diffuse reflection has random variations on the average a bias. In other words, while the specular reflection coefficient is a deterministic number depending on several unknown parameters, the diffuse reflection has a random nature. Generally, the sea surface is perturbed by small irregularities. Therefore, both reflection components are present. In practice, the specular reflective component has greater impact than the diffuse reflection and will cause a great angle measurement error. The impact of diffuse component is limited to oscillations which have little big deviation but it will reduce the angle measurement accuracy. According to test results, there are two big regional power drops during the test which are well predicted by the proposed model of the multipath effects. The results indicate that the first drop at about 2 km is mainly caused by the signal interference between the specular reflective component and direct wave component, while the second drop after 9 km is mainly because the target is far away and the signal is weaker.

6. CONCLUSIONS

A detailed model of the multipath propagation of low elevation target tracking using passive radars was presented in this paper. It had taken into account both types of reflections (the specular and the diffuse reflection components). The effect of multiple reflections from the sea surface was analyzed. Based on the geometry of the specular and the diffuse reflections, expressions for the reflection coefficient and the scattering field were derived. Experiments in the outfield indicate that the model proposed agrees with the test data well, which can provide an accurate prediction of the angle measurement errors in the presence of multipath effects. The result provides a reference to the detection and tracking of ship-borne radiation sources using anti-ship missile passive radar seekers.

REFERENCES

1. Beckmann, P. & Spizzichino, A. The scattering of electromagnetic waves from rough surfaces. Oxford: Pergamon Press, 1963.
2. Barton, D. K. Low-angle radar tracking. *Proc. IEEE*, 1974, **62**(6), 687-704.
3. Bruder, J.A. Multipath propagation effect on low-angle tracking at millimeter-wave frequencies. *IEE Proc. Radar Signal Proces.,* 1991, **138**(2), 172-84.
4. Sletten, M.A.; Trizna, D.B. & Hansen, J.P. Ultrawide-band radar observations of multipath propagation over the sea surface. *IEEE Trans. Antennas Propag.*, 1996, **44**(5), 646-651.
5. Bar-Shalom, Y.; Kumar, A.; Blair, W.D. & Groves, G.W. Tracking low elevation targets in the presence of multipath. *IEEE Trans. Aerosp. Electron. Syst.*, 1994, **30**(3), 973-79.
6. Blair, W.D.; Groves, G.W.; Bar-Shalom, Y. & Daeipour, E. Frequency agility and fusion for tracking targets in the presence of multipath propagation. *In* Proceedings of IEEE National Radar Conference, Atlanta, GA, US.

March 1994. pp. 166-170.

7. Daeipour, E.; Blair, W.D. & Bar-Shalom, Y. Bias compensation and tracking with monopulse radars in the presence of multipath. *IEEE Trans. Aerosp. Electron. Syst.*, 1997, **33**(3) pp. 863-882.

8. Chavali, P. & Nehorai, A. Cognitive radar for target tracking in multipath scenarios. *In* Proceedings of 2010 International Waveform Diversity and Design Conference, Niagara Falls, Canada, 2010. pp. 110-114.

9. Sen, S. & Nehorai, A. OFDM MIMO radar with mutual-information waveform design for low-grazing angle tracking. *IEEE Trans. Signal Proces.*, 2010, **58**(6), 3152-162.

10. Fabrizio, G. & Farina, A. Blind multipath separation for waveform recovery. *In* Proceedings of 2010 IEEE Radar Conference, Washington DC, USA , 2010, pp. 563-68.

11. Qian, W.; Qiao, X.; Zhu X. & Wei, Y. Multipath mitigation of low elevation for passive monopulse radar based on FrFT. *In* Proceedings of the First International Conference on Pervasive Computing, Signal Processing and Applications, Harbin, China, 2010. pp. 948-951.

12. Berizzi, F. & Dalle-Mese, E. Fractal analysis of the signal scattered from the sea surface. *IEEE Trans. Antennas Propag.*, 1999, **47**(2), 324-338.

13. Berizzi, F. & Dalle-Mese, E. Scattering from a 2-D sea fractal surface: fractal analysis of the scattered signal. *IEEE Trans. Antennas Propag.*, 2002, **50**(7), 912-25.

14. Yang, H. & Sun, J. Wave simulation based on ocean wave spectrums. *J. Syst. Simul.* (Chinese), 2002, **14**, 1175-178.

15. Beard, C.I. Coherent and incoherent scattering of microwaves from the ocean. *IEEE Trans. Antennas Propag.*, 1961, **9**(5), 470-83.

16. Barriek, D.E. Rough surface scattering based on the specular point theory. *IEEE Trans. Antennas Propag.*, 1968, **16**(4), 449-54.

Contributors

Dr Yuliang Qin received his MS and PhD (Information and Communication Engineering) from the National University of Defense Technology (NUDT), Changsha, China, in 2004 and 2008 respectively. He is currently working as an Associate Professor in the School of Electronic Science and Engineering, NUDT. His research interests are : Radar signal processing and radar systems.

Dr Yongqiang Cheng received his BS, MS, and PhD (Information and Communication Engineering) from NUDT, Changsha, China, in 2005, 2007, and 2012, respectively. He is currently working as a Lecturer at NUDT, China. His research interests include: Information geometry and statistical signal processing.